Constraints on lepton flavor violation in the MSSM
from the muon anomalous magnetic moment measurement

Z. Chacko[1] and Graham D. Kribs[2]

[1] *Department of Physics, Box 31560, University of Washington,*
Seattle, WA 98195

[2] *Department of Physics, University of Wisconsin,*
1150 University Ave., Madison, WI 53706-1390

zchacko@phys.washington.edu, kribs@pheno.physics.wisc.edu

Abstract

We establish a correspondence between those Feynman diagrams in the MSSM which give supersymmetric contributions to the muon anomalous magnetic moment and those which contribute to the flavor violating processes $\mu \to e\gamma$ and $\tau \to \mu\gamma$. Using current experimental limits on the branching ratios of these decay modes, combined with the assumption of a supersymmetric contribution to the muon anomalous magnetic moment, we establish bounds on the size of the lepton flavor violating soft masses in the MSSM largely independent of assumptions about other supersymmetric parameters. If the deviation measured at Brookhaven National Laboratory is from supersymmetry, we find the bounds $m^2{}_{e\mu}/\bar{m}^2 \lesssim 2 \times 10^{-4}$ and $m^2{}_{\tau\mu}/\bar{m}^2 \lesssim 1 \times 10^{-1}$, where $\bar{m}^2$ is the mass of the heaviest particle in any loop that contributes at this level to the anomalous magnetic moment of the muon. This provides a significant constraint on the non-flavor-blind mediation of supersymmetry breaking that often occurs at a suppressed level in many models, including gaugino mediation.

1   Introduction

The recent measurement [1] of the anomalous magnetic moment (g - 2) of the muon at BNL exhibits a deviation from what is expected from the Standard Model (SM) (for a clear review, see Ref. [2]). This suggests that a contribution from physics beyond the SM is necessary to explain the discrepancy. Supersymmetry has been known for some time to provide a significant contribution to anomalous magnetic moment operators [3, 4, 5, 6]. Several recent papers have also considered the possibility that the BNL measurement is evidence of a supersymmetric contribution to (g - 2) at the level of the experiment [7]. Other papers have also have considered a possible connection between muon (g - 2) and lepton flavor violation in both a supersymmetric [8] and nonsupersymmetric context [9]. In this paper we establish a correspondence between the supersymmetric diagrams in the MSSM that contribute to the anomalous magnetic moment of the muon and a precisely analogous class of diagrams that contribute to lepton flavor violating processes including $\mu \to e\gamma$ and $\tau \to \mu\gamma$. This enables us to place bounds on the flavor violating soft masses $m^2_{e\mu}$ and $m^2_{\tau\mu}$ in the MSSM. In particular we find $m^2_{e\mu}/\bar{m}^2 \leq 2 \times 10^{-4}$ and $m^2_{\tau\mu}/\bar{m}^2 \leq 1 \times 10^{-1}$, where $\bar{m}^2$ is the mass of the heaviest supersymmetric particle in any loop that contributes at this level to the anomalous magnetic moment of the muon. We do not assume any relation between the gaugino soft masses M_1, M_2, and the μ term in the superpotential, nor any relation among the slepton masses. The bounds we establish are largely insensitive to any supersymmetric parameters and assume only that there is no accidental cancellation between independent diagrams contributing to the flavor violating processes.

To understand the underlying reason for the correspondence between the diagrams for the two types of processes consider the structure of the relevant operators. The anomalous magnetic moment operator has the form

$$\mathcal{M}_\mu \quad = \quad \frac{ie}{2m_\mu}\overline{u}_\mu(p_2)a_\mu\sigma^{\mu\nu}q_\nu u_\mu(p_1)A_\mu \; . \tag{1}$$

The operator for the process $\mu \to e\gamma$ has the form

$$\mathcal{M}_{\mu e\gamma} \quad = \quad \frac{ie}{2m_\mu}\overline{u}_e(p_2)\sigma^{\mu\nu}q_\nu\left(a_l P_L + a_r P_R\right)u_\mu(p_1)A_\mu + h.c. \; , \tag{2}$$

where $P_{L,R} \equiv (1 \mp \gamma_5)/2$ and $\sigma^{\mu\nu} \equiv \frac{i}{2}\left[\gamma^\mu, \gamma^\nu\right]$. This has the same structure as the anomalous magnetic moment operator above provided $a_L = a_R$. In particular both operators involve a net chirality flip between the ingoing and outgoing leptons. This suggests that the different sets of graphs contributing to the two processes will have almost identical structures.

The complete expressions for the supersymmetric contributions to the muon anomalous magnetic moment have appeared in Refs. [4, 5, 6]. In general, muon (g - 2) arises from chargino-sneutrino and neutralino-smuon graphs, with contributions differing due to: the gaugino in the loop, the sfermion in the loop, and location of the chirality flip(s). In Figs. 1–6 we show the supersymmetric diagrams that give rise to muon (g - 2). In order to obtain the corresponding $\mu \to e\gamma$ graph for each of these diagrams we simply insert a flavor violating soft mass $m_{e\mu}{}^2$ along

the slepton line (other discussions of lepton flavor violation can be found in e.g., Refs. [10, 11, 12]). The resulting graph then gives an amplitude for $\mu \to e\gamma$ that is related in a straightforward way to the original amplitude for muon (g - 2) and also to the mass insertion $m_{e\mu}^2$. We can then use the upper limit on the branching ratio for the process $\mu \to e\gamma$ in the literature to obtain a bound on the flavor violating soft mass $m_{e\mu}^2$. This bound will of course be crucially dependent on the supersymmetric amplitude for muon (g - 2), which is an experimental input.

Naively one might think that these flavor violating diagrams may be heavily suppressed compared to the (g - 2) diagrams by a ratio of the electron mass to the muon mass or more since each (g - 2) graph depends explicitly on the (muon) flavor through one or more powers of the fermion mass (or the fermion Yukawa coupling), resulting in a very weak bound. However the detailed analysis we perform in subsequent sections reveals that this is *not* the case. We show that the supersymmetric contribution to (g -2) is dominated by graphs whose flavor violating analogues have no suppression factors, resulting in a very stringent bound.

Once constraints are established on the flavor violating mass mixing, they can be immediately applied to supersymmetry breaking models. Generally the constraints are most severe [12] in models that communicate supersymmetry breaking from a hidden sector through gravitational interactions [13]. In this framework the effective size of soft SUSY breaking is given by Planck suppressed operators such as

$$\int d^4\theta \frac{S^\dagger S}{M_{\mathrm{Pl}}^2} L_i^\dagger L_j \tag{3}$$

where S and $S^\dagger$ are hidden sector fields, while L_i and L_j are MSSM chiral multiplets of generation i and j. The Planck suppressed operators need not respect global flavor symmetries, and so i and j can be different. When the hidden sector fields acquire a SUSY breaking F-term the soft (mass)^2 generated is

$$\frac{|F_S|^2}{M_{\mathrm{Pl}}^2} \tag{4}$$

for all entries of the mass matrix in flavor space. Instead, current bounds on both quark and lepton flavor violating processes require either that the mass matrix is nearly diagonal, or that it is "aligned" to the Yukawa couplings. This is the supersymmetric flavor problem.

One solution is to push at least the first and second generation scalar masses to be very heavy (order tens of TeV or greater) [14], but this is inconsistent with generating a large supersymmetric contribution of (g - 2). Other methods of generating nearly flavor blind masses involve the gauge and gaugino fields in some nontrivial way. Gauge mediation [15] postulates that the dominant SUSY breaking is communicated to the MSSM through gauge interactions with a heavy messenger sector charged under the SM gauge group. Anomaly mediation [16] and gaugino mediation [17] postulate physically separating the hidden sector and the MSSM across a small extra dimension. Soft masses are generated for MSSM fields through either tree-level interactions (gaugino mediation) or at higher orders via the trace anomaly (anomaly mediation). In either case, the result is a nearly flavor blind soft mass spectrum.

3

Why then is SUSY breaking induced flavor violation important? We view this as means to test these mechanisms by accessing the flavor-nondiagonal structure. For instance, gravity mediation does contribute at a suppressed level to the soft SUSY breaking masses in gauge mediation, and so constraints on the size of flavor violating soft masses can be translated into upper bounds on the scale of supersymmetry breaking. Also, in both anomaly mediation and gaugino mediation there are exponentially suppressed flavor violating contributions resulting from the small wavefunction overlap on the visible brane of SUSY breaking fields localized on the hidden brane. The size of this suppressed contribution is

$$e^{-ML}\frac{|F|^2}{M^2} \tag{5}$$

where $M = (L^{-1}M_{\rm Pl}^2)^{1/3}$ is the effective Planck scale of the theory. Constraining the the size of flavor violation therefore restricts the size of the extra dimension, requiring it to be roughly an order of magnitude *larger* than the effective Planck length. Conversely, observing flavor violation in this framework would allow an estimate of the size of the extra dimension.

Why is *lepton* flavor violation important? The large body of evidence for neutrino oscillations shows that lepton number cannot be an exact symmetry of nature, and hence there is flavor physics that is outside the CKM matrix. Probing the sensitivity of the supersymmetry breaking sector to this flavor physics may provide insight into the scale and the nature of new flavor structure. It would be interesting to see how constraints on SUSY induced lepton flavor violation relate, if at all, to lepton violation through neutrino masses (e.g., see [18]). We leave this for further study.

This paper is organized as follows. In Sec. 2 we discuss the chargino-sneutrino contributions to (g - 2), and in Sec. 2.1 we calculate the chargino-sneutrino contribution to the lepton flavor violating process $\mu \to e\gamma$. We then use the current experimental bounds on the branching ratio into $\mu \to e\gamma$ to establish a bound on the sneutrino (left-left) $e \leftrightarrow \mu$ flavor mixing mass. In Sec. 3 we carry out the same analysis for the neutralino-slepton contributions, and obtain similar bounds on the left-left and right-right slepton flavor mixing masses between $e \leftrightarrow \mu$. In Sec. 4 we calculate the bounds on the flavor violating process $\tau \to \mu\gamma$. We find significantly weaker constraints on the $\mu \leftrightarrow \tau$ flavor mixing mass as compared with the $e \leftrightarrow \mu$ flavor mixing mass. Finally, in Sec. 5 we present our conclusions.

2   Chargino-sneutrino contributions

We begin by calculating the contributions to flavor violation resulting from sneutrino mixing. These are the analog processes to the sneutrino contributions to (g - 2). It is rather instructive to do this case analytically in detail, and so we restrict to considering $\tilde{\nu}_e - \tilde{\nu}_\mu$ mixing only.

Suppose a small flavor violating (mass)^2 $m_{12}^2 \ll m_{\tilde{\nu}_e, \tilde{\nu}_\mu}^2$ is added to the MSSM

$$\mathcal{L} = m_{\tilde{\nu}_e}^2 \tilde{\nu}_e^* \tilde{\nu}_e + m_{\tilde{\nu}_\mu}^2 \tilde{\nu}_\mu^* \tilde{\nu}_\mu + m_{12}^2 \tilde{\nu}_e^* \tilde{\nu}_\mu + h.c. , \tag{6}$$

4

giving a simple 2×2 mass matrix for the sneutrinos,

$$\mathcal{M}_{\tilde{\nu}}^2 = \begin{pmatrix} m_{\tilde{\nu}_e}^2 & m_{12}^2 \\ m_{12}^2 & m_{\tilde{\nu}_\mu}^2 \end{pmatrix} . \tag{7}$$

Note that we have absorbed the electroweak D-terms into our definition of $m_{\tilde{\ell}}^2$ for any $\ell = \tilde{\nu}_e, \tilde{\nu}_\mu, \tilde{e}, \tilde{\mu}$. Following the usual procedure we diagonalize this matrix, defining the mass eigenstates $\tilde{\nu}_{1,2}$ as

$$\begin{pmatrix} \tilde{\nu}_1 \\ \tilde{\nu}_2 \end{pmatrix} = \begin{pmatrix} \cos\theta_{\tilde{\nu}} & \sin\theta_{\tilde{\nu}} \\ -\sin\theta_{\tilde{\nu}} & \cos\theta_{\tilde{\nu}} \end{pmatrix} \begin{pmatrix} \tilde{\nu}_e \\ \tilde{\nu}_\mu \end{pmatrix} \tag{8}$$

ordered such that $\tilde{\nu}_1$ is the sneutrino that is majority $\tilde{\nu}_e$ (and $\tilde{\nu}_2$ is majority $\tilde{\nu}_\mu$). The sneutrino mass mixing angle is given by

$$\sin 2\theta_{\tilde{\nu}} = \frac{2m_{12}^2}{\sqrt{\left(m_{\tilde{\nu}_\mu}^2 - m_{\tilde{\nu}_e}^2\right)^2 + 4m_{12}^2}} \tag{9}$$

The interactions of the sneutrino mass eigenstates with charginos can be obtained by inserting the mass eigenstates into the interaction Lagrangian [19],

$$\mathcal{L} = \sum_k \Big[\overline{e}\left(-gP_R V_{k1} + P_L Y_e U_{k2}^*\right) \tilde{\chi}_k^c \left(\tilde{\nu}_1 \cos\theta_{\tilde{\nu}} - \tilde{\nu}_2 \sin\theta_{\tilde{\nu}}\right)$$
$$+ \overline{\mu}\left(-gP_R V_{k1} + P_L Y_\mu U_{k2}^*\right) \tilde{\chi}_k^c \left(\tilde{\nu}_1 \sin\theta_{\tilde{\nu}} + \tilde{\nu}_2 \cos\theta_{\tilde{\nu}}\right) \Big] + h.c. . \tag{10}$$

We now calculate the chargino-sneutrino contribution to (g - 2) in terms of the mass eigenstates. There are three distinct contributions that can be identified by the gaugino running in the loop and the location of the chirality flip: (a) pure gauge, (b) pure Higgsino, and (c) mixed, as shown in Figs. 1,2. [1] The total chargino-sneutrino contribution is simply

$$a_\mu = a_\mu^{(a)} + a_\mu^{(b)} + a_\mu^{(c)} , \tag{11}$$

where the individual diagrams give

$$\frac{16\pi^2}{m_\mu} a_\mu^{(a)} = \frac{m_\mu}{12 m_{\tilde{\chi}_k^\pm}^2} g_2^2 |V_{k1}|^2 \left[\sin^2\theta_{\tilde{\nu}} x_{k1} F_1^C(x_{k1}) + \cos^2\theta_{\tilde{\nu}} x_{k2} F_1^C(x_{k2}) \right] \tag{12}$$

$$\frac{16\pi^2}{m_\mu} a_\mu^{(b)} = \frac{m_\mu}{12 m_{\tilde{\chi}_k^\pm}^2} Y_\mu^2 |U_{k2}|^2 \left[\sin^2\theta_{\tilde{\nu}} x_{k1} F_1^C(x_{k1}) + \cos^2\theta_{\tilde{\nu}} x_{k2} F_1^C(x_{k2}) \right] \tag{13}$$

$$\frac{16\pi^2}{m_\mu} a_\mu^{(c)} = -\frac{2}{3 m_{\tilde{\chi}_k^\pm}} g_2 Y_\mu \text{Re}[V_{k1} U_{k2}] \left[\sin^2\theta_{\tilde{\nu}} x_{k1} F_2^C(x_{k1}) + \cos^2\theta_{\tilde{\nu}} x_{k2} F_2^C(x_{k2}) \right] , \tag{14}$$

where the sum over $k = 1, 2$ for the two charginos is implicitly understood. Here Y_μ is the muon Yukawa coupling, g_2 is the $SU(2)_L$ coupling, $x_{1k,2k} \equiv m_{\tilde{\chi}_k^\pm}^2 / m_{\tilde{\nu}_{1,2}}^2$, and U_{ij}, V_{ij} are the chargino

---

[1]These diagrams are in the interaction basis and are therefore schematic. However this is merely for purposes of clarity and does not affect our conclusions.

mixing matrices in the $(\tilde{W}^{\pm}, \tilde{H}^{\pm})$ basis. In the Appendix we provide the one-loop kinematical functions $F(x)$, which are defined identically to Ref. [6]. In the limit of no flavor violation, $m_{12}^2 \to 0$, this result agrees with previous calculations [5, 6].

Given that the size of flavor mixing mass is small, $m_{12}^2 \ll m_{\tilde{\nu}_e}^2, m_{\tilde{\nu}_\mu}^2$, there are two limiting cases: $m_{12}^2 \ll |m_{\tilde{\nu}_\mu}^2 - m_{\tilde{\nu}_e}^2|$, and $m_{12}^2 \gg |m_{\tilde{\nu}_\mu}^2 - m_{\tilde{\nu}_e}^2|$. In the first case, the mixing angle $\theta_{\tilde{\nu}} \ll 1$, so that $\cos\theta_{\tilde{\nu}} \simeq 1$ while $\sin\theta_{\tilde{\nu}} \ll 1$. The mass eigenstates are therefore nearly identical to the interaction eigenstates $\tilde{\nu}_2 \simeq \tilde{\nu}_\mu$ and $\tilde{\nu}_1 \simeq \tilde{\nu}_e$, so that Eqs. (12)–(14) trivially reduces to the interaction eigenstate result. In the second case, the mixing angle is maximal $\theta_{\tilde{\nu}} \simeq \pi/4$, so both sneutrinos contribute about equally but suppressed by a factor of $\sin^2\theta_{\tilde{\nu}} \simeq \cos^2\theta_{\tilde{\nu}} \simeq 1/2$. The sum of course gives nearly the same result as obtained without flavor mixing. Thus, our formalism gives the expected result that small flavor mixing in the sneutrino masses does not affect the prediction of (g - 2) in supersymmetry. We can express this result as

$$\sin^2\theta_{\tilde{\nu}} x_{k1} F_{1,2}^C(x_{k1}) + \cos^2\theta_{\tilde{\nu}} x_{k2} F_{1,2}^C(x_{k2}) \quad \simeq \quad x_{k,\mu} F_{1,2}^C(x_{k,\mu}) , \tag{15}$$

where $x_{k,\mu} \equiv m_{\chi_k^{\pm}}^2 / m_{\tilde{\nu}_\mu}^2$.

What is the relative size of each of these diagrams? Here the advantage of working in the interaction eigenstate basis is apparent. In the limit $M_2 \ll \mu$, the gaugino diagram dominates, and the others can be ignored. When $M_2 \sim \mu$, there is large gaugino-Higgsino mixing $|V_{k1}| \sim |U_{k2}|$, and so the relative size of the diagrams is governed by the couplings:

$$\left| a_\mu^{(a)} \right| : \left| a_\mu^{(b)} \right| : \left| a_\mu^{(c)} \right| \quad = \quad \left| \frac{g_2 m_\mu}{8 Y_\mu m_{\tilde{\chi}^{\pm}}} \right| : \left| \frac{Y_\mu m_\mu}{8 g_2 m_{\tilde{\chi}^{\pm}}} \right| : 1 . \tag{16}$$

In this case clearly diagram (b) is highly suppressed relative to diagram (a) or (c). The relative competition between diagram (a) and (c) depends on $\tan\beta$ and the mass of the chargino. Finally, the limit $\mu \ll M_2$ is slightly subtle. Fortunately it is straightforward to show that in this limit $|V_{k1} U_{k2}| \simeq \sqrt{2} M_W / M_2$, and so the ratio

$$\left| \frac{a_\mu^{(c)}}{a_\mu^{(b)}} \right| \quad \sim \quad \frac{g_2 \mu M_W}{Y_\mu m_\mu M_2} . \tag{17}$$

This ratio is much greater than one even for $\mu/M_2 = (m_\mu/M_W)^1 \sim 10^3$. Diagram (c) therefore dominates in the light Higgsino case.

Hence, the overwhelmingly dominant chargino-sneutrino contribution to (g - 2) arises from diagrams (a) and (c). Hereafter, we ignore diagram (b).

2.1   Flavor violating chargino-sneutrino graphs

The chargino-sneutrino contribution to lepton flavor violation is related to the muon (g - 2) graph by a simple replacement of the outgoing muon with an electron. The (g - 2) graphs can be written in pairs, with the same particles in the loop but the ingoing and outgoing muons

having different chiralities. These graphs have the same amplitude if there are no phases. For $\mu \to e\gamma$, however, there are two distinct sets of diagrams for the left-handed and right-handed incoming muons, leading to distinct contributions to the amplitude for a_l and a_r. We find that the contribution to a_l is suppressed by at least one additional power of the electron mass or electron Yukawa coupling, as so can be neglected. The contribution to a_r can be split into the same three contributions as we did above for (g - 2). We obtain

$$\frac{16\pi^2}{m_\mu} a_{\mu e\gamma}^{(a)} = \frac{m_\mu}{24 m_{\tilde\chi_k^\pm}^2} g_2^2 |V_{k1}|^2 \sin 2\theta_{\tilde\nu} \left[x_{k1} F_1^C(x_{k1}) - x_{k2} F_1^C(x_{k2}) \right] \tag{18}$$

$$\frac{16\pi^2}{m_\mu} a_{\mu e\gamma}^{(b)} = \frac{m_\mu}{24 m_{\tilde\chi_k^\pm}^2} Y_\mu Y_e |U_{k2}|^2 \sin 2\theta_{\tilde\nu} \left[x_{k1} F_1^C(x_{k1}) - x_{k2} F_1^C(x_{k2}) \right] \tag{19}$$

$$\frac{16\pi^2}{m_\mu} a_{\mu e\gamma}^{(c)} = -\frac{1}{3 m_{\tilde\chi_k^\pm}^2} g_2 Y_\mu \mathrm{Re}[V_{k1} U_{k2}] \sin 2\theta_{\tilde\nu} \left[x_{k1} F_2^C(x_{k1}) - x_{k2} F_2^C(x_{k2}) \right] . \tag{20}$$

Following the arguments we made for (g - 2), it is an excellent approximation to neglect diagram (b). The relationship between the amplitudes for (g - 2) and $\mu \to e\gamma$ can be seen by writing the ratio of diagrams (for fixed k, not summed over),

$$\frac{a_{\mu e\gamma}^{(i)}}{a_\mu^{(i)}} = \frac{1}{2} \frac{\sin 2\theta_{\tilde\nu} \left(x_{k1} F^C(x_{k1}) - x_{k2} F^C(x_{k2}) \right)}{x_{k,\mu} F^C(x_{k,\mu})} . \tag{21}$$

Here $F_1(x) = F_1^C(x)$ for $(i) = (a)$ and $F_1(x) = F_2^C(x)$ for $(i) = (c)$. Notice that the couplings and chargino mixing angle drops out. The expression can be evaluated (exactly) in the 2×2 mixing case. However before doing this we first obtain a qualitative understanding of this ratio of amplitudes.

From the expression above it is clear that unless

$$\frac{x_{k1} F^C(x_{k1})}{x_{k2} F^C(x_{k2})} - 1 \ll 1 \tag{22}$$

the ratio of amplitudes

$$\frac{a_{\mu e\gamma}^{(i)}}{a_\mu^{(i)}} \simeq \frac{1}{2} \sin 2\theta_{\tilde\nu} \simeq \frac{m_{12}^2}{\mathrm{Max}[m_{\tilde\nu_\mu}^2, m_{\tilde\nu_e}^2]} \tag{23}$$

Now the approximation (22) that leads to the equation above clearly breaks down in the limit $x_{k1} \to x_{k2}$. A careful examination of the structure of the functions $F^C(x)$ also shows that (22) is not satisfied when both $x_{k1} \gg 1$ and $x_{k2} \gg 1$ even if x_{k1} and x_{k2} are very different in magnitude. Since the functions $F^C(x)$ are monotonic apart from these regions the equation (22) is satisfied. We therefore examine these two limits in further detail.

We first consider the case of $x_{k1} \gg 1$, $x_{k2} \gg 1$. Then by studying the asymptotic behavior of $F^C(x)$ it follows that

$$\frac{a_{\mu e\gamma}^{(i)}}{a_\mu^{(i)}} \simeq \frac{m_{12}^2}{m_{\tilde\chi_k^\pm}^2} \tag{24}$$

This suggests that Eq. (22) can be generalized to

$$\frac{a_{\mu e\gamma}^{(i)}}{a_\mu^{(i)}} \simeq \frac{m_{12}^2}{\text{Max}[m_{\tilde{\nu}_\mu}^2, m_{\tilde{\nu}_e}^2, m_{\tilde{\chi}_k^\pm}^2]} \tag{25}$$

We now consider $x_{k1} \rightarrow x_{k2}$. For simplicity we examine the limits $|m_{\tilde{\nu}_\mu}^2 - m_{\tilde{\nu}_e}^2| \gg m_{12}^2$ and $|m_{\tilde{\nu}_\mu}^2 - m_{\tilde{\nu}_e}^2| \ll m_{12}^2$ separately. For $|m_{\tilde{\nu}_\mu}^2 - m_{\tilde{\nu}_e}^2| \gg m_{12}^2$ we have

$$\sin 2\theta_{\tilde{\nu}} \simeq \frac{2m_{12}^2}{|m_{\tilde{\nu}_\mu}^2 - m_{\tilde{\nu}_e}^2|} \tag{26}$$

and

$$\frac{x_{k1}F^C(x_{k1}) - x_{k2}F^C(x_{k2})}{x_{k,\mu}F^C(x_{k,\mu})} \simeq \frac{m_{\tilde{\nu}_\mu}^2 - m_{\tilde{\nu}_e}^2}{m_{\tilde{\nu}_\mu}^2} \qquad x_k \lesssim 1 \tag{27}$$

$$\frac{x_{k1}F^C(x_{k1}) - x_{k2}F^C(x_{k2})}{x_{k,\mu}F^C(x_{k,\mu})} \simeq \frac{m_{\tilde{\nu}_\mu}^2 - m_{\tilde{\nu}_e}^2}{m_{\tilde{\chi}_k^\pm}^2} \qquad x_k \gg 1 \tag{28}$$

up to numerical factors of order one. Combining these equations we find (25) is in fact reproduced even in this limit. Now consider the case $x_{k1} \rightarrow x_{k2}$ with $|m_{\tilde{\nu}_\mu}^2 - m_{\tilde{\nu}_e}^2| \ll m_{12}^2$. Then $\sin 2\theta_{\tilde{\nu}} \simeq 1$ while

$$\frac{x_{k1}F^C(x_{k1}) - x_{k2}F^C(x_{k2})}{x_{k,\mu}F^C(x_{k,\mu})} \simeq \frac{m_{12}^2}{m_{\tilde{\nu}_\mu}^2} \qquad x_k \lesssim 1 \tag{29}$$

$$\frac{x_{k1}F^C(x_{k1}) - x_{k2}F^C(x_{k2})}{x_{k,\mu}F^C(x_{k,\mu})} \simeq \frac{m_{12}^2}{m_{\tilde{\chi}_k^\pm}^2} \qquad x_k \gg 1 \tag{30}$$

Hence once again we find 25 holds. It is not difficult to verify that this remains true in the intermediate region $\left[|m_{\tilde{\nu}_\mu}^2 - m_{\tilde{\nu}_e}^2|\right] \approx m_{12}^2$. From this simple analysis we therefore conclude that the amplitudes for $\mu \rightarrow e\gamma$ and (g - 2) are simply related by

$$\frac{a_{\mu e\gamma}^{(i)}}{a_\mu^{(i)}} \simeq \frac{m_{12}^2}{\text{Max}[m_{\tilde{\nu}_\mu}^2, m_{\tilde{\nu}_e}^2, m_{\tilde{\chi}_k^\pm}^2]} \tag{31}$$

It is not difficult to understand the origin of this result. Given the correspondence between diagrams then elementary dimensional considerations indicate that the ratio of the two amplitudes is approximately given by $\frac{m_{12}^2}{M^2}$ where M^2 is a heavy scale. The most conservative assumption is that M^2 is the heaviest scale in the problem, the mass of the heaviest particle, which immediately yields Eq. (25).

We now perform a more careful analysis of the problem. The simplest piece of Eq. (21) to evaluate is the denominator. Since we are assuming no relations among the soft supersymmetry breaking masses, let's consider the three possible limits: (1) $x_{k,\mu} \gg 1$, (2) $x_{k,\mu} \sim 1$, and (3) $x_{k,\mu} \ll 1$, corresponding to the chargino mass being much greater than, roughly equal to, or

8

case	$a_{\mu e\gamma}^{(a)}/a_\mu^{(a)}$	$a_{\mu e\gamma}^{(c)}/a_\mu^{(c)}$
$x_{k,1}, x_{k,2} \gg 1$	$2m_{12}^2/m_{\tilde\chi_k^\pm}^2$	$m_{12}^2/m_{\tilde\chi_k^\pm}^2$
$x_{k,1}, x_{k,2} \ll 1$	$m_{12}^2/m_{\tilde\nu_e}^2$	$m_{12}^2/m_{\tilde\nu_e}^2$
$x_{k,1} \ll 1 \ll x_{k,2}$	$m_{12}^2/m_{\tilde\nu_e}^2$	$m_{12}^2/m_{\tilde\nu_e}^2$
$x_{k,2} \ll 1 \ll x_{k,1}$	$m_{12}^2/m_{\tilde\chi_k^\pm}^2$	$\frac{1}{2}m_{12}^2/(m_{\tilde\chi_k^\pm}^2 \ln m_{\tilde\nu_\mu}^2/m_{\tilde\chi_k^\pm}^2)$
$x_{k,1} \sim x_{k,2} \sim 1$	$\frac{2}{5}m_{12}^2/m_{\tilde\nu_e}^2$	$\frac{1}{4}m_{12}^2/m_{\tilde\nu_e}^2$
$x_{k,1} \sim 1,\ x_{k,2} \gg 1$	$\frac{1}{2}m_{12}^2/m_{\tilde\nu_e}^2$	$\frac{1}{3}m_{12}^2/m_{\tilde\nu_e}^2$
$x_{k,1} \sim 1,\ x_{k,2} \ll 1$	$\frac{1}{4}m_{12}^2/m_{\tilde\chi_k^\pm}^2$	$\frac{1}{3}m_{12}^2/(m_{\tilde\chi_k^\pm}^2 \ln m_{\tilde\nu_\mu}^2/m_{\tilde\chi_k^\pm}^2)$
$x_{k,2} \sim 1,\ x_{k,1} \gg 1$	$m_{12}^2/m_{\tilde\chi_k^\pm}^2$	$\frac{1}{2}m_{12}^2/m_{\tilde\chi_k^\pm}^2$
$x_{k,2} \sim 1,\ x_{k,1} \ll 1$	$m_{12}^2/m_{\tilde\nu_e}^2$	$m_{12}^2/m_{\tilde\nu_e}^2$

Table 1: The ratio of the amplitude for $\mu \to e\gamma$ over (g - 2) for diagram (a) and (c), for a given chargino (k fixed).

much smaller than the muon sneutrino mass, respectively. The limits of the one-loop functions are given in the Appendix, and so we simply state the result here:

$$\frac{2}{m_{\tilde\chi_k^\pm}^2} \qquad \text{for } x_{k,\mu} \gg 1 \tag{32}$$

$$\frac{1}{m_{\tilde\chi_k^\pm}^2}x_{k,\mu}F_1^C(x_{k,\mu}) \;=\; \frac{2}{m_{\tilde\nu_\mu}^2} \qquad \text{for } x_{k,\mu} \sim 1 \tag{33}$$

$$\frac{4}{m_{\tilde\nu_\mu}^2} \qquad \text{for } x_{k,\mu} \ll 1 , \tag{34}$$

which can be written very roughly as

$$\frac{1}{m_{\tilde\chi_k^\pm}^2}x_{k,\mu}F_1^C(x_{k,\mu}) \;\sim\; \frac{1}{\text{Max}[m_{\tilde\chi_k^\pm}^2, m_{\tilde\nu_\mu}^2]} \tag{35}$$

for any x, dropping overall factors of 2. The same expression can be found for the other one-loop functions with one exception.[2]

The numerator of Eq. (21) can also be evaluated for analogous limits. Since both sneutrino masses are in the expression there are nine distinct cases depending on the relative hierarchy of $m_{\tilde\nu_1}$, $m_{\tilde\nu_2}$, and $m_{\tilde\chi_k^\pm}$. The ratio can be evaluated straightforwardly in all of these cases. We present the results in Table 1. The tiny electron mass effect was ignored ($m_e/m_\mu \to 0$), and for those cases with $x_{i,k} \sim 1$ we have freely interchanged $m_{\tilde\nu_i}$ with $m_{\tilde\chi_k^\pm}$.

---

[2]The exception is the small x limit of $xF_2^C(x)$, which behaves as $-x\ln x$.

The most important result is that each (g - 2) diagram has a $\mu \to e\gamma$ counterpart that is proportional to

$$\delta_{12} = \frac{m_{12}^2}{\text{Max}[m_{\tilde{\chi}_k^\pm}^2, m_{\tilde{\nu}_e}^2, m_{\tilde{\nu}_\mu}^2]} \tag{36}$$

for *any* choice of soft breaking parameters. Right away we see that if a nonzero supersymmetric contribution to muon (g - 2) comes from mainly one diagram (with one chargino in the loop), then there is a prediction for the size of the lepton flavor violating process $\mu \to e\gamma$ that only depends on the size of the flavor mixing (mass)^2 divided by the larger of the chargino mass and the electron sneutrino mass.[3] The prediction is

$$a_{\mu e\gamma} \quad \gtrsim \quad \frac{1}{4} a_\mu \delta_{12} \simeq a_r \ . \tag{37}$$

We take the low value of $a_{\mu e\gamma}$ because we are interested in a bound. The width for $\mu \to e\gamma$ is easily obtained from the magnetic moment operator Eq. (2)

$$\Gamma(\mu \to e\gamma) \quad = \quad \frac{m_\mu e^2}{64\pi} \left(|a_l|^2 + |a_r|^2 \right) \ . \tag{38}$$

and as we discussed above, we may ignore the a_l contribution since it is further suppressed by the electron mass. The branching ratio is then

$$\text{BR}(\mu \to e\gamma) \quad = \quad \frac{3\pi^2 e^2}{G_F^2 m_\mu^4} |a_r|^2 \ . \tag{39}$$

which we can write as

$$\text{BR}(\mu \to e\gamma) \quad \simeq \quad 2.0 \times 10^{-4} \left(\frac{a_\mu}{4.3 \times 10^{-9}} \right)^2 \delta_{12}^2 \tag{40}$$

The current experimental bound is $\text{BR}(\mu \to e\gamma) < 1.2 \times 10^{-11}$ [20], which we can use to place a bound on the flavor mixing (mass)^2:

$$\delta_{12} < 2.4 \times 10^{-4} \left(\frac{\text{BR}(\mu \to e\gamma)}{1.2 \times 10^{-11}} \right)^{1/2} \left(\frac{4.3 \times 10^{-9}}{a_\mu} \right) \tag{41}$$

This bound is as accurate as δ_{12} is known, i.e., to within about a factor of 2.

3 Neutralino-slepton contributions

The second class of diagrams that contribute to muon (g - 2) and lepton flavor violation are ones with neutralinos and charged sleptons in the loop. We again restrict ourselves to $\mu \leftrightarrow e$ flavor transitions only, taking up other possibilities in Sec. 4. There are several important differences with the chargino-sneutrino contributions:

---

[3]In two of eighteen cases in Table 1 there is an additional logarithmic suppression of $1/\ln m_{\tilde{\chi}_k^\pm}^2/m_{\tilde{\nu}_\mu}^2$. However, the contribution to (g - 2) is suppressed as a power law $\propto m_{\tilde{\chi}_k^\pm}^2/m_{\tilde{\nu}_\mu}^2$, and so this case is not relevant to our discussion.

- there are four neutralinos $\tilde{B}$, $\tilde{W}^0$, $\tilde{H}_d^0$, and $\tilde{H}_u^0$ instead of two, and hence the mass matrix is four by four rather than two by two

- there is a pair of charged sleptons for each flavor $\tilde{e}_{L,R}$ and $\tilde{\mu}_{L,R}$

- left-right slepton mixing in addition to flavor mixing

- flavor mixing can be between left-left, right-right, a combination of both, and left-to-right or right-to-left

Unlike the chargino-sneutrino class of diagrams, there may be unsuppressed contribution to either a_l or a_r. We show the complete set of diagrams in Figs. 3–6. There is a nearly one-to-one correspondence between the contribution to a_l through left-left flavor mixing, and that for a_r through right-right flavor mixing (or vice versa). The exception are the diagrams with a Wino which couples only to left-handed fields.

As in the chargino-sneutrino case, roughly half of the diagrams are proportional to the electron mass or electron Yukawa coupling. Those diagrams that have an exact analog which simply replaces the electron mass with the muon mass can be safely neglected. This includes Figs. 3(e-R), 5(e-L), 5(g-L), 3(i-R), 5(i-L), 3(k-R), 5(k-L), 3(p-R), 5(p-L), and 5(r-L).

Neutralino-slepton contributions include a new set of diagrams resulting from left-right mixing between the sleptons. We have shown this set of diagrams separately in Figs. 4 and 6. Each muon (g - 2) diagram for a given muon chirality has *two* $\mu \to e\gamma$ contributions that result from the two possible orderings of the left-to-right transition and the flavor transition. One of these orderings involves muon left-right mixing whereas the other involves electron left-right mixing. (Only the muon left-right mixing is shown in Figs. 4 and 6.) Ordinarily the flavor-diagonal slepton mass matrix is written as

$$
\mathcal{M}_{\tilde{\ell}}^2 \;\; = \;\; \begin{pmatrix} m_{\tilde{\ell}_L}^2 & m_\ell(-\mu\tan\beta + A_\ell) \\ m_\ell(-\mu\tan\beta + A_\ell) & m_{\tilde{\ell}_R}^2 \end{pmatrix} \tag{42}
$$

As long as the different flavor A-terms are not as hierarchically different as the lepton masses, the diagrams with electron left-right mixing can be neglected. Even though we will assume this in what follows it is clear that weakening this restriction will not affect the bound.

The final class of diagrams to be considered are those with *only* a Higgsino in the loop. In (g - 2), it is straightforward to show that there are always larger contributions from either mixed gaugino/Higgsino diagrams or from pure gaugino diagrams. We may safely neglect the diagrams Figs. 3(h-R) and 5(h-L) in favor of 3(j-L) and 5(j-R), respectively. This is because the Bino content of the lightest neutralino goes as $N_{11} \simeq \sin\theta_W M_Z/M_1$ (and the Wino content goes as $N_{12} \simeq \cos\theta_W M_Z/M_2$). The Higgsino diagram is proportional to $m_\mu Y_\mu^2 |N_{13}|^2$, whereas the mixed Higgsino/Bino contribution is proportional to $m_{\tilde{\chi}_1^0} g_1 Y_\mu N_{11} N_{13}$. So long as $\sin\theta_W M_Z/M_1 \gtrsim m_\mu Y_\mu/(m_{\tilde{\chi}_1^0} g_1)$, the small Bino content of the lightest neutralino dominates the amplitude. This is precisely analogous to neglecting the Higgsino diagram in favor of the mixed Higgsino/Wino diagram for the chargino-sneutrino contribution.

The Higgsino diagrams with left-right mixing, Figs. 4(n-R) and 6(n-L), are somewhat more subtle in the limit $\mu \ll M_1, M_2$. In these two diagrams, the chirality flip is on the internal line, with $\tan\beta$ enhanced left-right mixing on the slepton line. However these graphs can be neglected relative to 4(m-R) and 6(m-L) so long as the ratio of the Bino mass to the Higgsino mass is less than about $(g_1/Y_\mu)^2$. Therefore neglecting this diagram relative to the others is consistent in all but highly fine-tuned regions of parameter space.

Interestingly, the remaining contributions to a_r and a_l depend exclusively on the left-left flavor changing transition mass $m_{12}^{LL\,2}$ and the right-right flavor changing transition mass $m_{12}^{RR\,2}$. Hence, there is essentially no interference between the amplitudes involving a left-left flavor changing transition with the right-right flavor changing transition.

In general, the charged slepton mass matrix takes the form

$$
\mathcal{M}_{\tilde\ell}^2 \;=\; \begin{pmatrix} \bar m_{e_L}^2 & m_e(A_e - \mu\tan\beta) & \bar m^2{}_{12}^{LL} & \\ m_e(A_e - \mu\tan\beta) & \bar m_{e_R}^2 & & \bar m^2{}_{12}^{RR} \\ \bar m^2{}_{12}^{LL} & & \bar m_{\mu_R}^2 & m_\mu(A_\mu - \mu\tan\beta) \\ & \bar m^2{}_{12}^{RR} & m_\mu(A_\mu - \mu\tan\beta) & \bar m_{\mu_L}^2 \end{pmatrix} \tag{43}
$$

This 4×4 matrix must be diagonalized to carry out an exact calculation. We wish to exploit the ease of computing in the 2×2 case. We can achieve this by first diagonalizing the upper left and bottom right (2×2) blocks of this matrix individually. As long as we are working in the one flavor violating insertion limit then this problem reduces to that of several (2×2) matrices which can be handled independently.

So, we decompose the $4x4$ matrix into [4]

$$
\mathcal{M}_{\tilde\ell_L}^2 \;=\; \begin{pmatrix} m_{e_L}^2 & m_{12}^{LL\,2} \\ m_{12}^{LL\,2} & m_{\mu_L}^2 \end{pmatrix} \quad , \quad \mathcal{M}_{\tilde\ell_R}^2 \;=\; \begin{pmatrix} m_{e_R}^2 & m_{12}^{RR\,2} \\ m_{12}^{RR\,2} & m_{\mu_R}^2 \end{pmatrix} \tag{44}
$$

It is important to note that the elements of these matrices are not exactly those of the original mass matrix we started with, i.e. m_{e_L} is now not the mass of the left handed slepton in the original mass matrix but the mass of the eigenstate which is 'mostly' the original left handed slepton. Similarly m_{12}^{LL} here is simply the mass in the corresponding position of the mass matrix after the (2×2) blocks have been diagonalized. The resulting matrices can be easily diagonalized just like the chargino-sneutrino case, resulting in the "mass eigenvalues" $m_{\tilde\ell_{1,2}^L}$, $m_{\tilde\ell_{1,2}^R}$ and mixing angles $\theta_{\tilde\ell L}$, $\theta_{\tilde\ell R}$.

Using our treatment for left-right mixing, we can now write the contribution to the (g - 2) amplitude for those diagrams with unsuppressed $\mu \to e\gamma$ analogs:

$$
\frac{16\pi^2}{m_\mu} a_\mu^{(d-R)} \;\simeq\; -\frac{m_\mu}{24 m_{\tilde\chi_k^0}^2} g_1^2 |N_{k1}|^2 x_{k,L} F_1^N(x_{k,L}) \tag{45}
$$

[4]Other possible decompositions exist, but this one suffices for the purpose of establishing a bound.

$$\frac{16\pi^2}{m_\mu}a_\mu^{(f-R)} \simeq -\frac{m_\mu}{24m_{\tilde\chi_k^0}^2}g_2^2|N_{k2}|^2 x_{k,L}F_1^N(x_{k,L}) \tag{46}$$

$$\frac{16\pi^2}{m_\mu}a_\mu^{(g-R)} \simeq -\frac{m_\mu}{12m_{\tilde\chi_k^0}^2}g_1g_2\mathrm{Re}[N_{k1}N_{k2}^*]x_{k,L}F_1^N(x_{k,L}) \tag{47}$$

$$\frac{16\pi^2}{m_\mu}a_\mu^{(j-R)} \simeq \frac{1}{3\sqrt2 m_{\tilde\chi_k^0}}g_1Y_\mu\mathrm{Re}[N_{k1}N_{k3}]x_{k,L}F_2^N(x_{k,L}) \tag{48}$$

$$\frac{16\pi^2}{m_\mu}a_\mu^{(l-R)} \simeq \frac{1}{3\sqrt2 m_{\tilde\chi_k^0}}g_2Y_\mu\mathrm{Re}[N_{k2}N_{k3}]x_{k,L}F_2^N(x_{k,L}) \tag{49}$$

$$\frac{16\pi^2}{m_\mu}a_\mu^{(m-R)} \simeq \frac{m_\mu(A_\mu-\mu\tan\beta)}{3m_{\tilde\mu_R}^2 m_{\tilde\chi_k^0}}g_1^2\mathrm{Re}[N_{k1}N_{k1}]x_{k,L}F_2^N(x_{k,L}) \tag{50}$$

$$\frac{16\pi^2}{m_\mu}a_\mu^{(o-R)} \simeq \frac{m_\mu(A_\mu-\mu\tan\beta)}{3m_{\tilde\mu_R}^2 m_{\tilde\chi_k^0}}g_1g_2\mathrm{Re}[N_{k1}N_{k2}]x_{k,L}F_2^N(x_{k,L}) \tag{51}$$

$$\frac{16\pi^2}{m_\mu}a_\mu^{(q-R)} \simeq -\frac{\sqrt2 m_\mu^2(A_\mu-\mu\tan\beta)}{3m_{\tilde\mu_R}^2 m_{\tilde\chi_k^0}^2}g_1Y_\mu\mathrm{Re}[N_{k1}N_{k3}^*]x_{k,L}F_1^N(x_{k,L}) \tag{52}$$

$$\frac{16\pi^2}{m_\mu}a_\mu^{(r-R)} \simeq -\frac{\sqrt2 m_\mu^2(A_\mu-\mu\tan\beta)}{3m_{\tilde\mu_R}^2 m_{\tilde\chi_k^0}^2}g_2Y_\mu\mathrm{Re}[N_{k2}N_{k3}^*]x_{k,L}F_1^N(x_{k,L}) \tag{53}$$

and

$$\frac{16\pi^2}{m_\mu}a_\mu^{(d-L)} \simeq -\frac{m_\mu}{6m_{\tilde\chi_k^0}^2}g_1^2|N_{k1}|^2 y_{k,R}F_1^N(y_{k,R}) \tag{54}$$

$$\frac{16\pi^2}{m_\mu}a_\mu^{(j-L)} \simeq \frac{\sqrt2}{3m_{\tilde\chi_k^0}}g_1Y_\mu\mathrm{Re}[N_{k1}N_{k3}]y_{k,R}F_2^N(y_{k,R}) \tag{55}$$

$$\frac{16\pi^2}{m_\mu}a_\mu^{(m-L)} \simeq \frac{\sqrt2 m_\mu(A_\mu-\mu\tan\beta)}{3m_{\tilde\mu_L}^2 m_{\tilde\chi_k^0}}g_1^2\mathrm{Re}[N_{k1}N_{k1}]y_{k,R}F_2^N(y_{k,R}) \tag{56}$$

$$\frac{16\pi^2}{m_\mu}a_\mu^{(o-L)} \simeq \frac{\sqrt2 m_\mu(A_\mu-\mu\tan\beta)}{3m_{\tilde\mu_L}^2 m_{\tilde\chi_k^0}}g_1g_2\mathrm{Re}[N_{k1}N_{k2}]y_{k,R}F_2^N(y_{k,R})\ . \tag{57}$$

$$\frac{16\pi^2}{m_\mu}a_\mu^{(q-L)} \simeq -\frac{2\sqrt2 m_\mu^2(A_\mu-\mu\tan\beta)}{3m_{\tilde\mu_L}^2 m_{\tilde\chi_k^0}^2}g_1Y_\mu\mathrm{Re}[N_{k1}N_{k3}^*]y_{k,R}F_1^N(y_{k,R}) \tag{58}$$

where the sum over $k=1,2,3,4$ for the four neutralinos is implicitly understood. Here g_1 is the U(1)$_Y$ coupling, $x_{k,L}\equiv m_{\tilde\chi_k^0}^2/m_{\tilde\mu_L}^2$, $y_{k,R}\equiv m_{\tilde\chi_k^0}^2/m_{\tilde\mu_R}^2$, and N_{ij} is the neutralino mixing matrix in the $(\tilde B,\tilde W^0,\tilde H_d^0,\tilde H_u^0)$ basis. The one-loop kinematical functions $F(x)$ are defined identically to Ref. [6] and are given in the Appendix.

The contribution to $\mu\to e\gamma$ can be obtained from the above amplitudes by replacing

$$x_{k,L}F_i^N(x_{k,L}) \longrightarrow \frac12\sin2\theta_{\tilde\ell L}\left(x_{k,1}F_i^N(x_{k,1})-x_{k,2}F_i^N(x_{k,2})\right) \tag{59}$$

$$y_{k,R}F_i^N(y_{k,R}) \longrightarrow \frac12\sin2\theta_{\tilde\ell R}\left(y_{k,1}F_i^N(y_{k,1})-y_{k,2}F_i^N(y_{k,2})\right)\ , \tag{60}$$

13

case	$a_{\mu e\gamma}/a_\mu$ (set 1)	$a_{\mu e\gamma}/a_\mu$ (set 2)
$x_{k,1}, x_{k,2} \gg 1$	$-\frac{11}{2}m_{12}^2/m_{\tilde\chi_k^0}^2$	$-3m_{12}^2/m_{\tilde\chi_k^0}^2$
$x_{k,1}, x_{k,2} \ll 1$	$m_{12}^2/m_{\tilde e^L}^2$	$m_{12}^2/m_{\tilde e^L}^2$
$x_{k,1} \ll 1 \ll x_{k,2}$	$m_{12}^2/m_{\tilde e^L}^2$	$m_{12}^2/m_{\tilde e^L}^2$
$x_{k,2} \ll 1 \ll x_{k,1}$	$2m_{12}^2/m_{\tilde\chi_k^0}^2$	$m_{12}^2/m_{\tilde\chi_k^0}^2$
$x_{k,1} \sim x_{k,2} \sim 1$	$\frac{3}{5}m_{12}^2/m_{\tilde e^L}^2$	$\frac{1}{2}m_{12}^2/m_{\tilde e^L}^2$
$x_{k,1} \sim 1,\, x_{k,2} \gg 1$	$\frac{3}{4}m_{12}^2/m_{\tilde e^L}^2$	$\frac{2}{3}m_{12}^2/m_{\tilde e^L}^2$
$x_{k,1} \sim 1,\, x_{k,2} \ll 1$	$\frac{1}{2}m_{12}^2/m_{\tilde\chi_k^0}^2$	$\frac{1}{3}m_{12}^2/m_{\tilde\chi_k^0}^2$
$x_{k,2} \sim 1,\, x_{k,1} \gg 1$	$3m_{12}^2/m_{\tilde\chi_k^0}^2$	$2m_{12}^2/m_{\tilde\chi_k^0}^2$
$x_{k,2} \sim 1,\, x_{k,1} \ll 1$	$m_{12}^2/m_{\tilde e^L}^2$	$m_{12}^2/m_{\tilde e^L}^2$

Table 2: The ratio of the amplitude for $\mu \to e\gamma$ over (g - 2), for a given neutralino (fixed k), for two classes of diagrams. Set 1: Fig. 3(d-R),(f-R),(g-R), and Fig 4(q-R),(r-R) and Set 2: Fig. 3(j-R),(l-R) and 4(m-R),(o-R). The same results hold for $x \leftrightarrow y$ $m_{\tilde\ell L}^2 \leftrightarrow m_{\tilde\ell R}^2$, and $m_{12}^{LL\,2} \leftrightarrow m_{12}^{RR\,2}$, where Set 1 is just Fig. 5(d-L), Fig. 6(q-L) and Set 2 includes Fig. 5(j-L), Fig. 6(m-L) and (o-L).

where $x_{k,\{1,2\}} \equiv m_{\tilde\chi_k^0}^2/m_{\tilde\ell_{\{1,2\}}^L}^2$ and $y_{k,\{1,2\}} \equiv m_{\tilde\chi_k^0}^2/m_{\tilde\ell_{\{1,2\}}^R}^2$. This is completely analogous to the chargino-sneutrino result. In fact, the ratio of any pair of diagrams for a given neutralino (fixed k) is the same:

$$\frac{a_{\mu e\gamma}^{(R)}}{a_\mu^{(R)}} = \frac{1}{2}\sin 2\theta_{\tilde\ell L}\frac{x_{k,1}F_i^N(x_{k,1}) - x_{k,2}F_i^N(x_{k,2})}{x_{k,L}F_i^N(x_{k,L})} \tag{61}$$

$$\frac{a_{\mu e\gamma}^{(L)}}{a_\mu^{(L)}} = \frac{1}{2}\sin 2\theta_{\tilde\ell R}\frac{y_{k,1}F_i^N(y_{k,1}) - y_{k,2}F_i^N(y_{k,2})}{y_{k,R}F_i^N(y_{k,R})} \tag{62}$$

Following the same arguments used the chargino-sneutrino case, we obtain

$$\frac{a_{\mu e\gamma}^{(R)}}{a_\mu^{(R)}} \simeq \frac{m_{12}^{LL\,2}}{\mathrm{Max}[m_{\tilde\mu_L}^2, m_{\tilde e_L}^2, m_{\tilde\chi_k^0}^2]} \tag{63}$$

$$\frac{a_{\mu e\gamma}^{(L)}}{a_\mu^{(L)}} \simeq \frac{m_{12}^{RR\,2}}{\mathrm{Max}[m_{\tilde\mu_R}^2, m_{\tilde e_R}^2, m_{\tilde\chi_k^0}^2]}\,. \tag{64}$$

Just as in the chargino-sneutrino case, the ratio can be calculated exactly in various limits shown in Table 2. The results in the table closely match the expectation above. From this, we can predict the size of the amplitude for $\mu \to e\gamma$ assuming that muon (g - 2) is dominated by one diagram (with one neutralino). Either

$$a_{\mu e\gamma}^r \gtrsim \frac{1}{3}a_\mu\delta_{12}^{LL} \tag{65}$$

or

$$a^l_{\mu e \gamma} \gtrsim \frac{1}{3} a_\mu \delta^{RR}_{12} \, , \tag{66}$$

Following the same analysis in the chargino-sneutrino sector, we can use the current experimental bound on the branching ratio for $\mu \to e\gamma$ to obtain a bound on the flavor mixing (mass)^2:

$$\delta^{LL}_{12} < 1.8 \times 10^{-4} \left(\frac{\mathrm{BR}(\mu \to e\gamma)}{1.2 \times 10^{-11}} \right)^{1/2} \left(\frac{4.3 \times 10^{-9}}{a_\mu} \right) \tag{67}$$

or

$$\delta^{RR}_{12} < 1.8 \times 10^{-4} \left(\frac{\mathrm{BR}(\mu \to e\gamma)}{1.2 \times 10^{-11}} \right)^{1/2} \left(\frac{4.3 \times 10^{-9}}{a_\mu} \right) \tag{68}$$

Combining the chargino-sneutrino results with the neutralino-slepton results, we obtain roughly the same result given above. Notice that, without making assumptions about the soft mass hierarchy, the best we can do is to place a bound on δ^{LL}_{12} or δ^{RR}_{12}, but not both simultaneously.

4 Other lepton flavor violating decays

We now consider constraints on the flavor violating transition $\tau \to \mu\gamma$. Once again we can establish a correspondence between the various diagrams. Diagrams which have a chirality flip on the external τ line or have a tau Yukawa vertex have an m_τ/m_μ amplitude enhancement which is not there in the $\mu \to e\gamma$ decay. The (g - 2) graphs can be written in pairs, with the same particles in the loop but the ingoing and outgoing muons having different chiralities. At least one of the graphs in each pair is always enhanced with the exception of $[a_\mu{}^{m-R}$ and $a_\mu{}^{m-L}]$, $[a_\mu{}^{o-R}$ and $a_\mu{}^{o-L}]$. These graphs are not enhanced unless we assume that A_l is generation independent and hence the off diagonal elements in the slepton mass matrix are proportional to the Yukawa couplings. From now on we will assume that this is the case and proceed. Writing the relevant part of the interaction Lagrangian as

$$\mathcal{M} = \frac{ie}{2m_\mu} \overline{u}_\mu(p_2) \sigma^{\mu\nu} q_\nu \left(a_l P_L + a_r P_R \right) u_\tau(p_1) A_\mu + \mathrm{h.c.} \tag{69}$$

In analogy with the $\mu \to e\gamma$ the smallest value of a_l or a_r corresponding to this process is approximately given by

$$a = \frac{1}{4} a_\mu \frac{m_\tau}{m_\mu} \frac{m_{23}{}^2}{\bar{m}^2} \tag{70}$$

The width is given by

$$\Gamma(\mu \to e\gamma) \;\; = \;\; \frac{m_\tau{}^3 e^2}{64\pi m_\mu{}^2} \left(|a_l|^2 + |a_r|^2 \right) \, . \tag{71}$$

15

Using the experimental bound on the branching ratio ($\leq 1.1 \times 10^{-6}$) [21] and from the the lifetime of the τ (2.9×10^{-13}s) we obtain

$$\frac{m_{23}{}^2}{\bar{m}^2} \leq 1.4 \times 10^{-1} \tag{72}$$

5 Conclusions

We have found a precise correspondence between the supersymmetric diagrams that contribute to the muon anomalous magnetic moment and those which contribute to the flavor violating processes $\mu \to e\gamma$ and $\tau \to \mu\gamma$. Using current experimental limits on the branching ratios of these decay modes, combined with the assumption of a supersymmetric contribution to the muon anomalous magnetic moment, we have found strong bounds on the size of the $e \leftrightarrow \mu$ lepton flavor violating soft mass, essentially independent of assumptions other supersymmetric parameters. Assuming the current deviation measured at BNL is from supersymmetry, and using the current experimental limits on radiative leptonic branching ratios, we find $m^2_{e\mu}/\bar{m}^2 \lesssim 2 \times 10^{-4}$ and $m^2_{\tau\mu}/\bar{m}^2 \lesssim 1 \times 10^{-1}$, where $\bar{m}^2$ is the mass of the heaviest particle in any loop that contributes at this level to the anomalous magnetic moment of the muon. Improvement in the experimental measurement of (g - 2) can be easily incorporated into our results since our bound is inversely proportional to the central value discrepancy between the standard model and experiment.

The absence of lepton flavor violation places a significant constraint on the non-flavor-blind mediation of supersymmetry breaking that often occurs at a suppressed level in many models. Finding lepton flavor violation, however, could lead to fascinating ways of accessing aspects of supersymmetry breaking models that are not easily obtained through other means, such as estimating the size of the extra dimension in anomaly mediation or gaugino mediation models.

Note added: As this paper was being completed, another paper recently appeared [22] that also discussed the connection between lepton flavor violation and muon (g - 2), with similar conclusions.

Acknowledgments

Appendix: One-loop kinematical functions and their limits.

The kinematical functions $F(x)$ that arise in muon (g - 2) and the lepton flavor violating processes $\ell_i \to \ell_j \gamma$ are given by [6]

$$F_1^C(x) = \frac{2}{(1-x)^4}\left[2 + 3x - 6x^2 + x^3 + 6x\ln x\right] \tag{73}$$

$$F_2^C(x) = -\frac{3}{2(1-x)^3}\left[3 - 4x + x^2 + 2\ln x\right] \tag{74}$$

$$F_1^N(x) = \frac{2}{(1-x)^4}\left[1 - 6x + 3x^2 + 2x^3 - 6x^2\ln x\right] \tag{75}$$

$$F_2^N(x) = \frac{3}{(1-x)^3}\left[1 - x^2 + 2x\ln x\right] \; . \tag{76}$$

There are three interesting regions of these functions: small x, $x \sim 1$, and large x. In the small x limit, $xF(x)$ can be written as

$$xF_1^C(x) = 4x + 22x^2 + \ldots \tag{77}$$

$$xF_2^C(x) = 3x\ln 1/x - \frac{9}{2}x - \frac{15}{2}x^2 + \ldots \tag{78}$$

$$xF_1^N(x) = 2x - 4x^2 + \ldots \tag{79}$$

$$xF_2^N(x) = 3x + 9x^2 + \ldots \; . \tag{80}$$

For $x \sim 1$, $xF(x)$ can be written as

$$xF_1^C(x) = 1 + \frac{2}{5}(x-1) - \frac{1}{5}(x-1)^2 + \ldots \tag{81}$$

$$xF_2^C(x) = 1 + \frac{1}{4}(x-1) - \frac{3}{20}(x-1)^2 + \ldots \tag{82}$$

$$xF_1^N(x) = 1 + \frac{3}{5}(x-1) - \frac{1}{5}(x-1)^2 + \ldots \tag{83}$$

$$xF_2^N(x) = 1 + \frac{1}{2}(x-1) - \frac{1}{5}(x-1)^2 + \ldots \; . \tag{84}$$

Finally, in the large x limit, $xF(x)$ can be written as

$$xF_1^C(x) = 2 - \frac{4}{x} - \frac{22}{x^2} + \ldots \tag{85}$$

$$xF_2^C(x) = \frac{3}{2} - \frac{3}{2x} - \frac{9}{2x^2} + \ldots \tag{86}$$

$$xF_1^N(x) = 4 + \frac{22}{x} + \frac{52}{x^2} + \ldots \tag{87}$$

$$xF_2^N(x) = 3 + \frac{9}{x} + \frac{15}{x^2} + \ldots \; . \tag{88}$$

References

[1] H. N. Brown *et al.* [Muon g-2 Collaboration], Phys. Rev. Lett. **86**, 2227 (2001) [hep-ex/0102017].

[2] A. Czarnecki and W. J. Marciano, hep-ph/0102122;

[3] P. Fayet, in "Unification Of The Fundamental Particle Interactions." edited by S. . Ferrara, J. . Ellis and P. . Van Nieuwenhuizen, *New York, Usa, Plenum (1980)*; J. A. Grifols and A. Mendez, Phys. Rev. D **26**, 1809 (1982); J. Ellis, J. Hagelin and D. V. Nanopoulos, Phys. Lett. B **116**, 283 (1982); R. Barbieri and L. Maiani, Phys. Lett. B **117**, 203 (1982).

[4] T. Moroi, Phys. Rev. D **53**, 6565 (1996) [Erratum-ibid. D **56**, 4424 (1996)] [hep-ph/9512396].

[5] M. Carena, G. F. Giudice and C. E. Wagner, Phys. Lett. B **390**, 234 (1997) [hep-ph/9610233].

[6] S. P. Martin and J. D. Wells, hep-ph/0103067.

[7] Ref. [2];

L. Everett, G. L. Kane, S. Rigolin and L. Wang, hep-ph/0102145;

J. L. Feng and K. T. Matchev, hep-ph/0102146;

E. A. Baltz and P. Gondolo, hep-ph/0102147;

U. Chattopadhyay and P. Nath, hep-ph/0102157;

S. Komine, T. Moroi and M. Yamaguchi, hep-ph/0102204;

first paper in Ref. [8];

J. Ellis, D. V. Nanopoulos and K. A. Olive, hep-ph/0102331;

R. Arnowitt, B. Dutta, B. Hu and Y. Santoso, hep-ph/0102344;

K. Choi, K. Hwang, S. K. Kang, K. Y. Lee and W. Y. Song, hep-ph/0103048;

J. E. Kim, B. Kyae and H. M. Lee, hep-ph/0103054;

Ref. [6];

S. Komine, T. Moroi and M. Yamaguchi, hep-ph/0103182;

K. Cheung, C. Chou and O. C. Kong, hep-ph/0103183;

S. Baek, P. Ko and H. S. Lee, hep-ph/0103218;

A. Bartl, T. Gajdosik, E. Lunghi, A. Masiero, W. Porod, H. Stremnitzer and O. Vives, hep-ph/0103324;

second paper in Ref. [8];

F. Richard, hep-ph/0104106;

third paper in Ref. [8];

C. Chen and C. Q. Geng, hep-ph/0104151;

K. Enqvist, E. Gabrielli and K. Huitu, hep-ph/0104174.

[8] J. Hisano and K. Tobe, hep-ph/0102315;

 D. F. Carvalho, J. Ellis, M. E. Gomez and S. Lola, hep-ph/0103256;

 S. Baek, T. Goto, Y. Okada and K. Okumura, hep-ph/0104146.

[9] T. Huang, Z. H. Lin, L. Y. Shan and X. Zhang, hep-ph/0102193;

 E. Ma and M. Raidal, hep-ph/0102255;

 Z. Xing, hep-ph/0102304;

 X. Calmet, H. Fritzsch and D. Holtmannspotter, hep-ph/0103012;

 R. A. Diaz, R. Martinez and J. A. Rodriguez, hep-ph/0103050;

 S. K. Kang and K. Y. Lee, hep-ph/0103064;

 E. Mituda and K. Sasaki, hep-ph/0103202.

[10] M. J. Duncan, Nucl. Phys. B **221**, 285 (1983); J. F. Donoghue, H. P. Nilles and D. Wyler, Phys. Lett. B **128**, 55 (1983).

[11] S. Dimopoulos and D. Sutter, Nucl. Phys. B **452**, 496 (1995) [hep-ph/9504415]; D. W. Sutter, hep-ph/9704390.

[12] F. Gabbiani, E. Gabrielli, A. Masiero and L. Silvestrini, Nucl. Phys. B **477**, 321 (1996) [hep-ph/9604387].

[13] For a review, see H. P. Nilles, Phys. Rept. **110**, 1 (1984).

[14] M. Drees, Phys. Rev. D **33**, 1468 (1986); M. Dine, A. Kagan and S. Samuel, Phys. Lett. B **243**, 250 (1990); S. Dimopoulos and G. F. Giudice, Phys. Lett. B **357**, 573 (1995) [hep-ph/9507282]; A. Pomarol and D. Tommasini, Nucl. Phys. B **466**, 3 (1996) [hep-ph/9507462]; A. G. Cohen, D. B. Kaplan and A. E. Nelson, Phys. Lett. B **388**, 588 (1996) [hep-ph/9607394].

[15] M. Dine and A. E. Nelson, Phys. Rev. D **48**, 1277 (1993) [hep-ph/9303230]; M. Dine, A. E. Nelson and Y. Shirman, Phys. Rev. D **51**, 1362 (1995) [hep-ph/9408384]; M. Dine, A. E. Nelson, Y. Nir and Y. Shirman, Phys. Rev. D **53**, 2658 (1996) [hep-ph/9507378].

[16] L. Randall and R. Sundrum, Nucl. Phys. B **557**, 79 (1999) [hep-th/9810155]; G. F. Giudice, M. A. Luty, H. Murayama and R. Rattazzi, JHEP **9812**, 027 (1998) [hep-ph/9810442].

[17] D. E. Kaplan, G. D. Kribs and M. Schmaltz, Phys. Rev. D **62**, 035010 (2000) [hep-ph/9911293]; Z. Chacko, M. A. Luty, A. E. Nelson and E. Ponton, JHEP **0001**, 003 (2000) [hep-ph/9911323].

[18] J. L. Feng, Y. Nir and Y. Shadmi, Phys. Rev. D **61**, 113005 (2000) [hep-ph/9911370].

[19] J. F. Gunion and H. E. Haber, Nucl. Phys. B **272**, 1 (1986) [Erratum-ibid. B **402**, 1 (1986)].

[20] M. L. Brooks *et al.* [MEGA Collaboration], Phys. Rev. Lett. **83**, 1521 (1999) [hep-ex/9905013].

[21] S. Ahmed et. al., CLEO collaboration, Phys. Rev. D61, 071101 (2000)

[22] M. Graesser and S. Thomas, hep-ph/0104254.
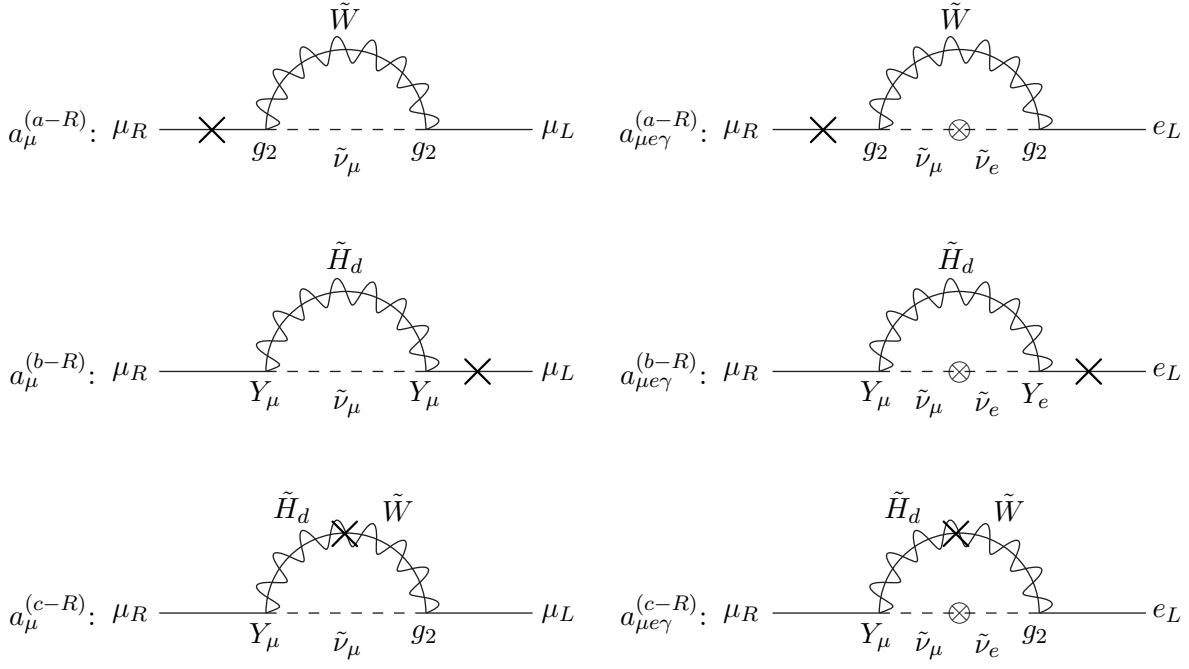
Figure 1: Chargino-sneutrino contributions to a_r that give rise to muon $g - 2$ and $\mu \to e\gamma$ in the interaction eigenstate basis. The photon (not shown) is emitted from the chargino. The chirality flip is shown by the $\times$ on the fermion line, while the the lepton flavor violating mass insertion is shown by the $\otimes$.

Figure 2: Similar to Fig. 2, the chargino-sneutrino contributions to a_l that give rise to muon $g-2$ and $\mu \to e\gamma$ in the interaction eigenstate basis.

Figure 3: Neutralino-slepton contributions to a_r that give rise to muon $g-2$ and $\mu \to e\gamma$ in the interaction eigenstate basis. The photon (not shown) is emitted from the slepton. The chirality flip is shown by a $\times$ on the fermion line and the slepton flavor violating mass insertion is shown by a $\otimes$.
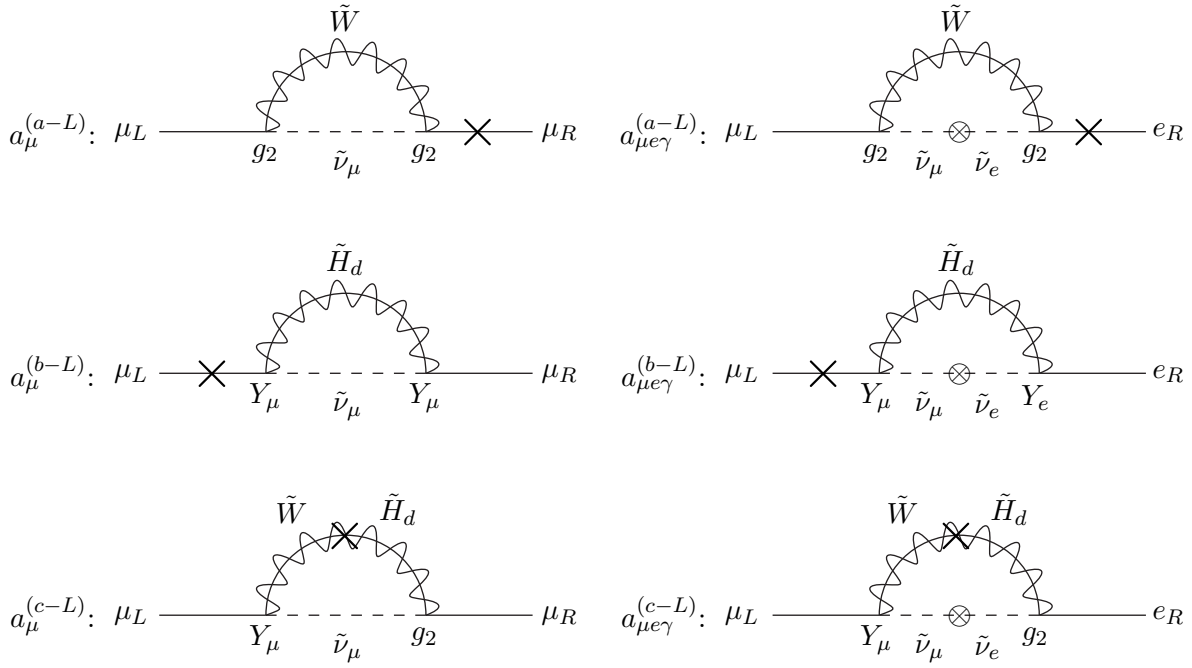
Figure 4: Similar to Fig. 3, the neutralino-slepton contributions to a_r with a left-right slepton mass insertion that give rise to muon $g-2$ and $\mu \to e\gamma$ in the interaction eigenstate basis are shown. The slepton left-right mass insertion is shown by a •.
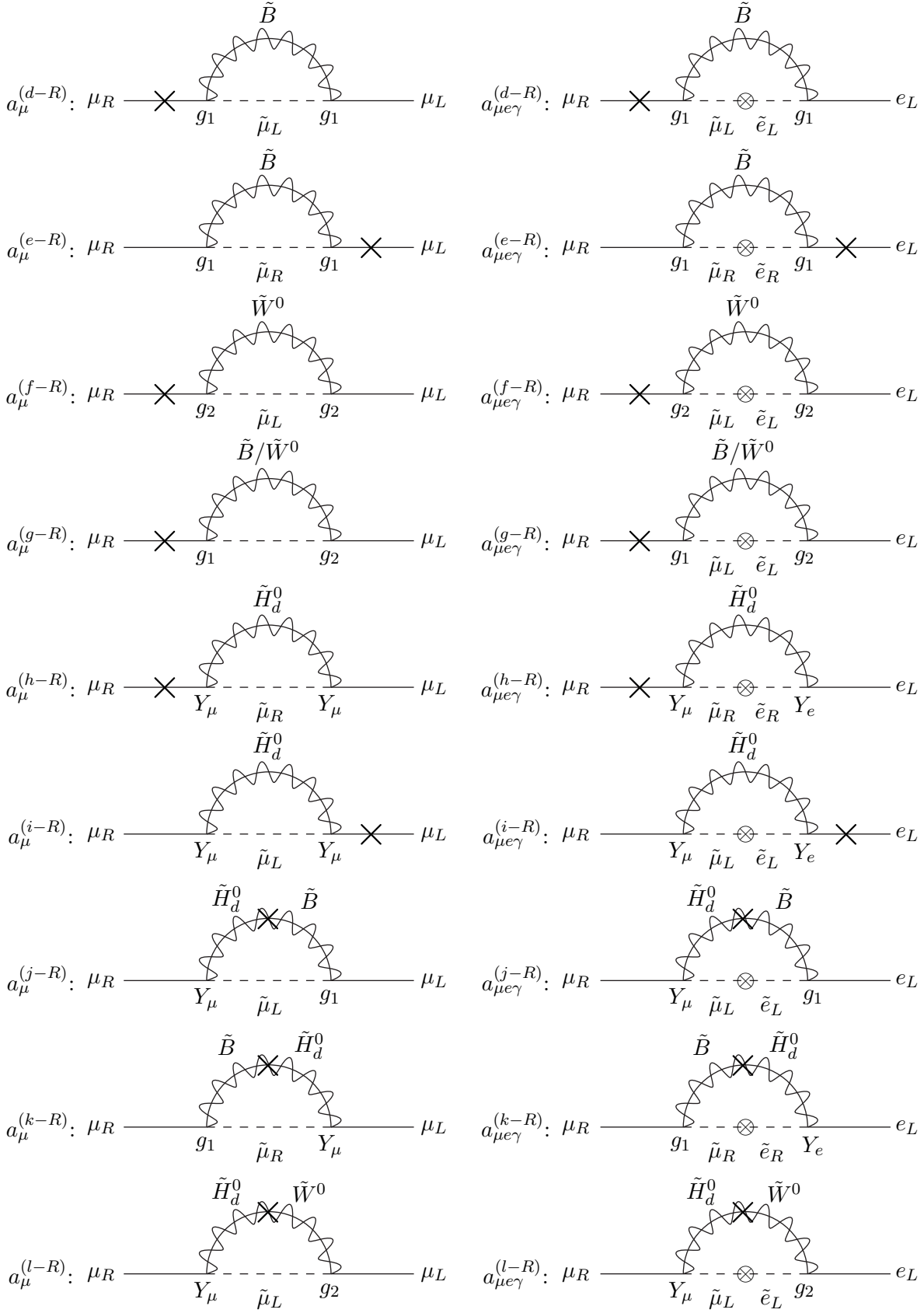
Figure 5: Neutralino-slepton contributions to a_l that give rise to muon $g-2$ and $\mu \to e\gamma$ in the interaction eigenstate basis. The chirality flip is shown by a $\times$ on the fermion line and the slepton flavor violating mass insertion is shown by a $\otimes$.

25

$a_\mu^{(m-L)}$: μ_L — g_1 $\tilde{\mu}_L$ $\tilde{\mu}_R$ g_1 — μ_R, with $\tilde{B}$

$a_{\mu e\gamma}^{(m-L-\mu)}$: μ_L — g_1 $\tilde{\mu}_L$ $\tilde{\mu}_R$ $\tilde{e}_R$ g_1 — e_R, with $\tilde{B}$

$a_\mu^{(n-L)}$: μ_L — Y_μ $\tilde{\mu}_R$ $\tilde{\mu}_L$ Y_μ — μ_R, with $\tilde{H}_d^0$

$a_{\mu e\gamma}^{(n-L-\mu)}$: μ_L — Y_μ $\tilde{\mu}_R$ $\tilde{\mu}_L$ $\tilde{e}_L$ Y_e — e_R, with $\tilde{H}_d^0$

$a_\mu^{(o-L)}$: μ_L — g_1 $\tilde{\mu}_L$ $\tilde{\mu}_R$ g_2 — μ_R, with $\tilde{W}^0$ $\tilde{B}$

$a_{\mu e\gamma}^{(o-L-\mu)}$: μ_L — g_1 $\tilde{\mu}_L$ $\tilde{\mu}_R$ $\tilde{e}_R$ g_2 — e_R, with $\tilde{W}^0$ $\tilde{B}$

$a_\mu^{(p-L)}$: μ_L — Y_μ $\tilde{\mu}_R$ $\tilde{\mu}_L$ g_1 — μ_R, with $\tilde{H}_d^0/\tilde{B}$

$a_{\mu e\gamma}^{(p-L)}$: μ_L — Y_μ $\tilde{\mu}_R$ $\tilde{\mu}_L$ $\tilde{e}_L$ g_1 — e_R, with $\tilde{H}_d^0/\tilde{B}$

$a_\mu^{(q-L)}$: μ_L — Y_μ $\tilde{\mu}_L$ $\tilde{\mu}_R$ g_1 — μ_R, with $\tilde{H}_d^0/\tilde{B}$

$a_{\mu e\gamma}^{(q-L)}$: μ_L — Y_μ $\tilde{\mu}_L$ $\tilde{\mu}_R$ $\tilde{e}_R$ g_1 — e_R, with $\tilde{H}_d^0/\tilde{B}$

$a_\mu^{(r-L)}$: μ_L — Y_μ $\tilde{\mu}_R$ $\tilde{\mu}_L$ g_2 — μ_R, with $\tilde{W}/\tilde{H}_d^0$

$a_{\mu e\gamma}^{(r-L)}$: μ_L — Y_μ $\tilde{\mu}_R$ $\tilde{\mu}_L$ $\tilde{e}_L$ g_2 — e_R, with $\tilde{W}/\tilde{H}_d^0$
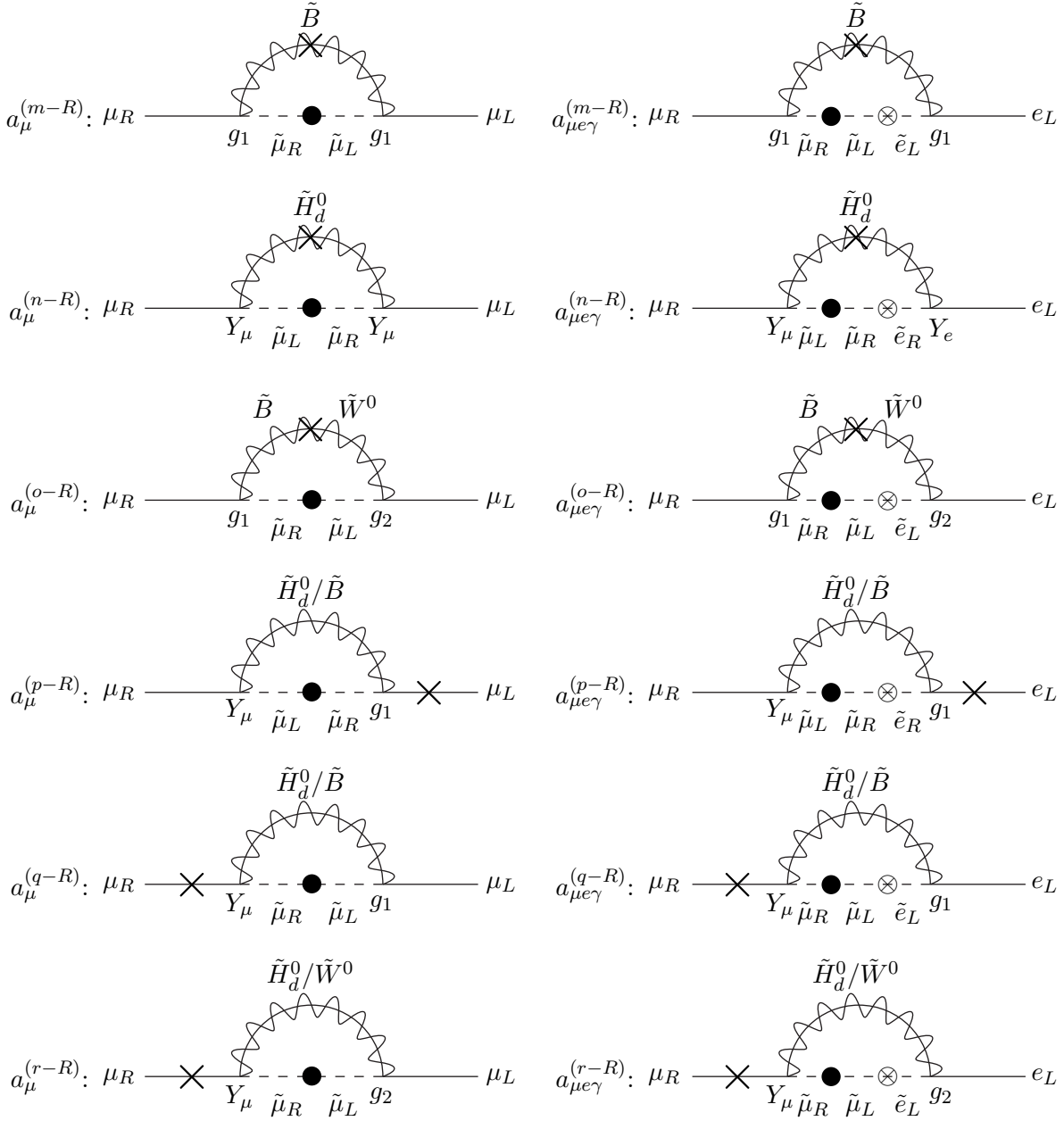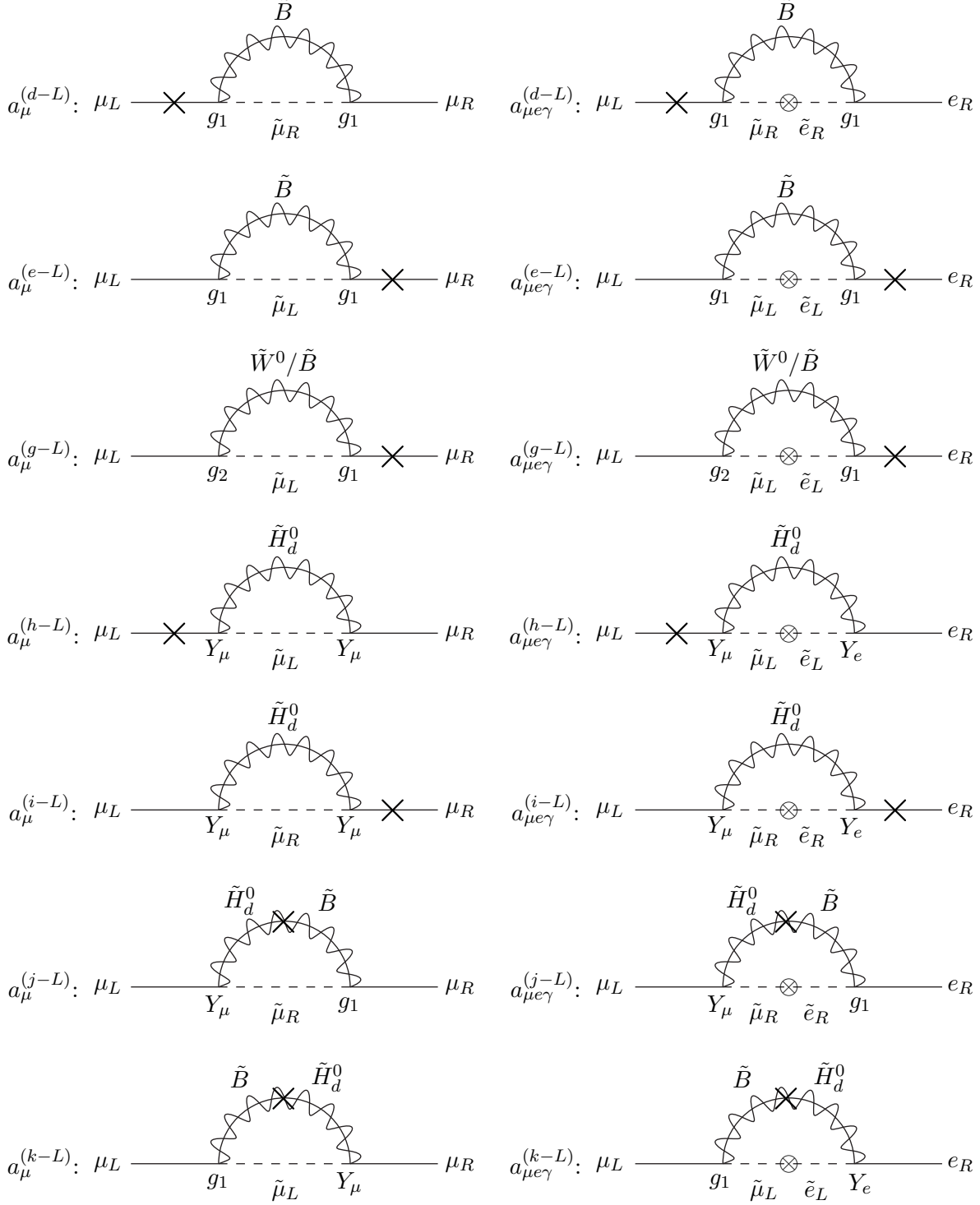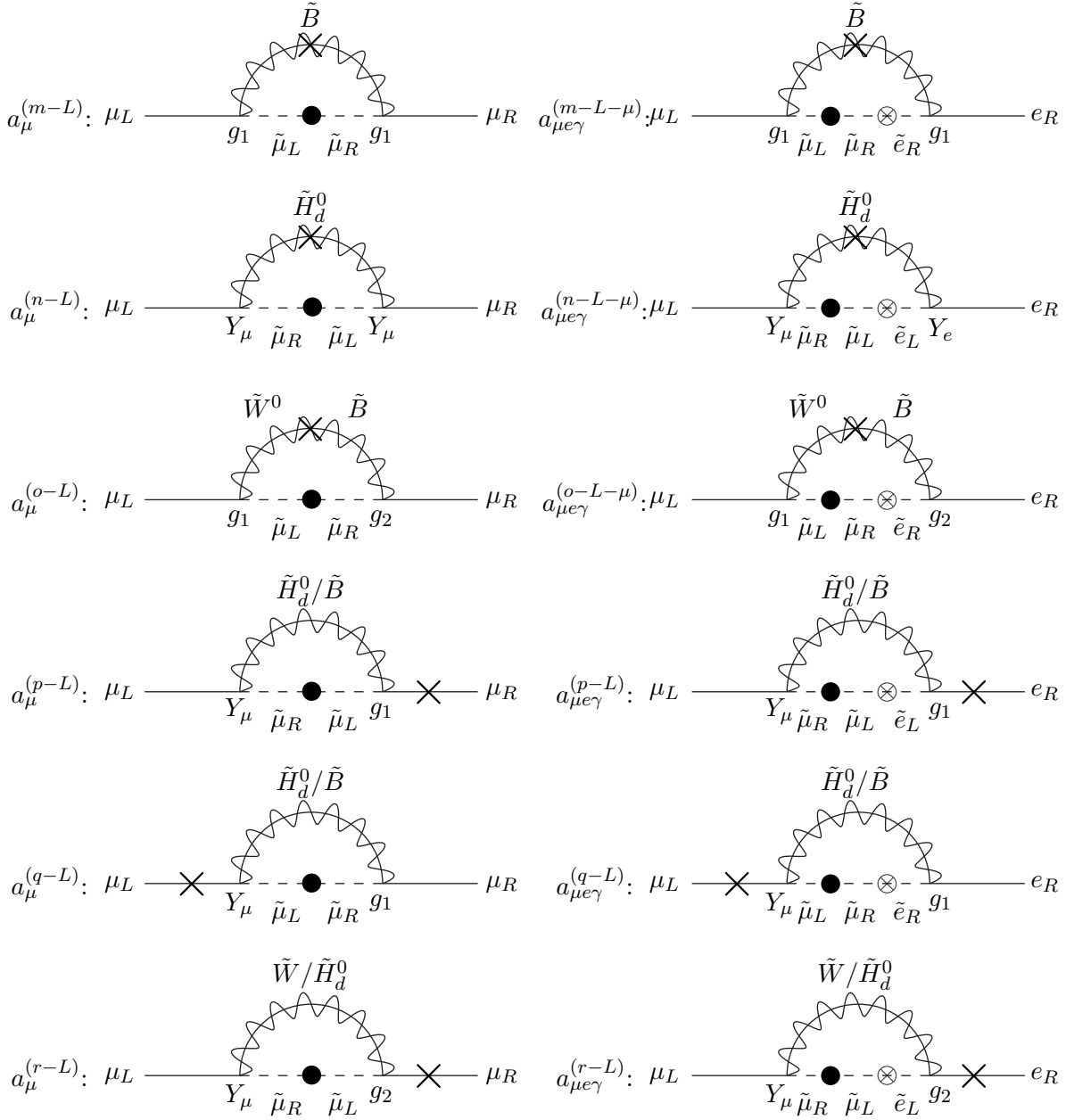
Figure 6: Similar to Fig. 5, the neutralino-slepton contributions to a_l with a left-right slepton mass insertion that give rise to muon $g-2$ and $\mu \to e\gamma$ in the interaction eigenstate basis are shown. The slepton left-right mass insertion is shown by a •.